ISSN 2047-0371

3.4.5. Glacier Movement

C. Scott Watson[1] and Duncan Quincey[1]
[1] School of Geography and water@leeds, University of Leeds (scott@www.rockyglaciers.co.uk)

ABSTRACT: Quantification of glacier movement can supplement measurements of surface elevation change to allow an integrated assessment of glacier mass balance. Glacier velocity is also closely linked to the surface morphology of both clean-ice and debris-covered glaciers. Velocity applications include distinguishing active from inactive ice on debris-covered glaciers, identifying glacier surge events, or inferring basal conditions using seasonal observations. Surface displacements can be surveyed manually in the field using trigonometric principles and a total station or theodolite for example, or dGPS measurements, which allow horizontal and vertical movement to be quantified for accessible areas. Semi-automated remote sensing techniques such as feature tracking (using optical or radar imagery) and interferometric synthetic aperture radar (InSAR) (using radar imagery), can provide spatially distributed and multi-temporal velocity fields of horizontal glacier surface displacement. Remote-sensing techniques are more practical and can provide a greater distribution of measurements over larger spatial scales. Time-lapse imagery can also be exploited to track surface displacements, providing fine temporal and spatial resolution, although the latter is dependent upon the range between camera and glacier surface. This chapter outlines the costs, benefits, and methodological considerations when using field-based and remote sensing techniques for deriving glacier velocity, and example workflows are presented.

KEYWORDS: glacier velocity, feature tracking, SAR interferometry, time-lapse, surge

Introduction

Glacier movement is spatially and temporally variable, both within glacierised catchments, and between glacierised regions, determined by topographic and climatic conditions. Quantifying movement rates in conjunction with mass balance estimates, helps reveal the response of glacial environments to climate change. Glacier movement can be decoupled from climatic warming, such as during sudden surge events where rapid displacement can occur over a short period, or enhanced glacial retreat that can be initiated at lacustrine- or marine-terminating glaciers. Assessing the future evolution and mass balance of glaciers is essential to determine their contribution to sea level change, seasonal meltwater availability including supra-, en-, sub- and pro-glacial water storage, and glacial lake outburst flood (GLOF) hazard development.

Glacier movement can be attributed to basal sliding, internal ice deformation, and subglacial deformation of the glacier bed; hence there is an interaction between the gravitational driving force of downward ice movement, and the resistance encountered at the bed and margins (Benn and Evans, 2010). Difficulties in accessing the ice-bed interface of a glacier makes quantifying basal movement difficult, though not impossible (e.g. Hubbard, 2002; Kavanaugh and Clarke, 2006) hence glacier surface movement is commonly used as a proxy to represent overall glacier motion. Therefore, methods of quantifying glacier surface movement form the focus of this chapter.

Geomorphological interest

As an agent of significant landscape change, glacier movement and stagnation, both past and present, is of notable interest to geomorphologists at local to regional scales.

Examples include reconstructing past glacial extents (e.g. Benn and Owen, 2002; Nesje, 2009), assessing the proglacial implications of GLOF events following glacial recession and subsequent lake development (e.g. Westoby *et al.,* 2014), and examining glacial morphology and dynamics such as during surge events (e.g. Clarke *et al.*, 1984; Kamb *et al.*, 1985; Quincey *et al.*, 2011), or on debris-covered glaciers exhibiting stagnation and surface lowering (e.g. Immerzeel *et al.*, 2014). The contemporary response of ice sheets to climate change is also receiving significant attention owing to the implications for sea level rise and the potential for resource exploitation. Here, ice movement reflects the export and subsequent loss of ice mass into the ocean, which is coupled to surface meltwater fluxes (Zwally *et al.*, 2002). The likely response of ice sheets during deglaciation can be inferred from interpretations of deglaciated landscapes (e.g. the BRITICE mapping project) (Evans *et al.*, 2005), and used in conjunction with numerical modelling to assess contemporary ice sheet change (Bingham *et al.*, 2010).

Debris-covered glaciers

Assessments of glacier movement are important when studying debris-covered glaciers owing to a complex response to climate change. Debris-covered glaciers that are stagnating and exhibiting surface lowering are associated with the development of supraglacial ponds (Bolch *et al.*, 2012). The thermal energy stored in ponds and transmitted to the underlying glacier ice can locally increase ablation, and under favourable conditions ponds can also coalesce into larger glacial lakes with subsequent water storage and potentially hazardous implications (Benn *et al.*, 2012). Exposed ice faces often surround supraglacial ponds and can represent areas of enhanced ablation in a melt regime that is largely suppressed by thick debris cover (Sakai *et al.*, 2002; Reid and Brock, 2014). Here, the persistence and evolution of both supraglacial ponds and ice cliffs are closely linked to a low glacier velocity (Quincey *et al.*, 2007).

Surge glaciers

Surge glaciers are characterised by an oscillatory behaviour which switches between a long quiescent phase (decades to years) and a short active phase (years to decades) of rapid ice movement, where velocities can be ca. 100 times greater (Meier and Post, 1969). These events can bias snap-shot mass balance and glacial extent observations if not accounted for. However, over longer periods this effect may be diminished: Gardelle *et al.* (2013) observed similar mass budgets for surge-type and non-surging glaciers in the Pamir-Karakorum Himalaya over a 10 year period. The spatial and temporal change in glacier velocity during a surge can be observed using remote sensing techniques (e.g. Quincey et al., 2011) (Figure 1), which can help describe the distribution, duration, magnitude, and return period of glacier surges, for which the controlling mechanisms are not fully understood. Evidence of past surge-type behaviour can be derived from characteristic deformation landforms such as thrust moraines, concertina eskers (Evans and Rea, 1999), or deformed medial moraines on the contemporary glacier surface (Meier and Post, 1969).

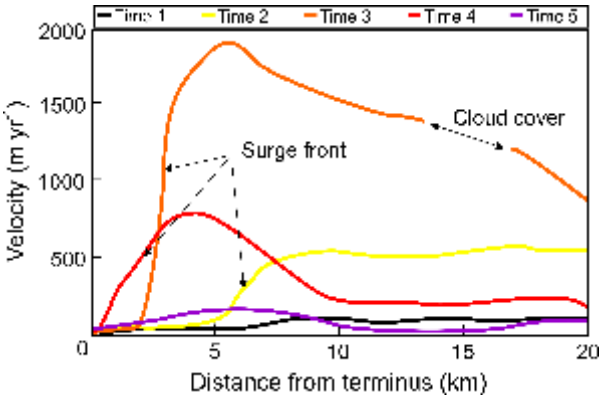

Figure 1: Illustrative propagation of a glacier surge front derived from centre line surface velocities from Quincey et al. (2011). Note that areas of cloud cover or poor image contrast can lead to data voids.

Observations of glacier movement

Glacier movement is associated with erosional and depositional landforms, and the transport of sediment down glaciated catchments. This can be important for contemporary glacier dynamics, such as a terminal moraine-dammed lake promoting calving retreat (e.g. Imja Tsho, Nepal), and can also be used to interpret and reconstruct past glacial landscapes. Water-occupied

over-deepened basins epitomise glacial erosion and subsequent glacial retreat.

Seasonal velocity observations can indicate basal thermal conditions. For example, contrasting summer and winter velocities suggest meltwater driven basal sliding is likely, which is linked to bed erosion and ultimately landscape evolution. Studies investigating glacier movement over shorter temporal timescales (e.g. hours, days, and weeks) than is common for remotely sensed observations are able to identify the links between glacier-hydrology and glacier velocity. Seasonal meltwater input into a glacier system can act to reduce basal drag and subsequently increase horizontal and vertical glacier velocity as the sub-glacial drainage system evolves (e.g. Mair *et al.*, 2001; Copland *et al.*, 2003). Hence the water pressure in this drainage system is closely linked to glacier sliding (Iken *et al.*, 1983). This increase in velocity can be short-lived where a subglacial meltwater reservoir outbursts (e.g. Bingham *et al.*, 2006). Depleted surface meltwater inputs and increasing channelization of the drainage system subsequently reduces subglacial water pressure. However, horizontal velocities may remain raised compared to winter in response to continued meltwater input, despite a more effective drainage system (Bingham *et al.*, 2006).

Summary of techniques

Early observations of glacier movement utilised transects of stakes inserted into the glacier surface, which can be tracked from surrounding moraines using a theodolite and triangulation techniques (e.g. Kodama and Mae, 1976). Alternatively, increasingly utilised remote sensing techniques can enable a fully distributed analysis of glacier surface movement both horizontally and vertically (Quincey *et al.*, 2005), which complements geomorphological observations (e.g. Hambrey *et al.*, 2008), and allows an integrated assessment of glacier dynamics alongside mass balance observations (e.g. Benn *et al.*, 2012).

Table 1. A summary of techniques for assessing glacier surface motion and practical considerations.

Technique	Costs	Benefits	Considerations
Manual survey	• dGPS, total station or theodolite • > 1 field visit usually required	• Sub-metre accuracy (sub-centimetre with certain dGPS setups) • Horizontal and vertical displacement information • Point measurements of velocity, rather than an average for a pixel/ cell (e.g. feature tracking) • Sub-daily temporal resolution possible	• Site accessibility • Selecting appropriate visible and persistent markers on a debris-covered surface • Spatial coverage on the order of several km^2 depending upon terrain • The NERC Geophysical Equipment has a range of survey equipment available for loan
Time-lapse survey	• Several cameras generally required • dGPS survey of reference targets • > 1 field visit usually required	• Sub-metre accuracy • Horizontal and vertical displacement information • Ancillary information e.g. weather conditions • Sub-daily temporal resolution possible with the overall mission duration limited by battery power (typically < 1 year)	• Number and position of cameras (considering site accessibility) • Surface shadows • Cloud or snow cover obscuring targets/ rain on the lens • Restricting camera movement e.g. bolting down the enclosure • Waterproofing of the camera and battery life/ ancillary solar power • Camera theft • Spatial coverage dependent upon camera quality and viewpoint elevation. Typically < 0.5 km^2 per camera
Feature tracking	• Software access and training • Imagery costs	• Automated workflows • Dense velocity field coverage • Glacier-scale spatial coverage	• Imagery choice: optical or SAR • Imagery spatial and temporal resolution (see Figure 2). Unmanned Aerial Vehicle imagery could be sub-daily. However, more commonly used satellite imagery will be on the order of days to months. • Cloud covered scenes/ poor image contrast on optical imagery • Software choice/ processing algorithm
SAR interferometry	• Technically more challenging than feature tracking	• Automated workflows • Higher precision than is achievable using feature tracking with optical or SAR imagery • Very small displacements are detectable	• The revisit period of imagery relative to the estimated glacier displacement in order to preserve coherence

Commonly used remote sensing techniques for assessing glacier surface movement include manual surveys, time-lapse camera surveys, satellite image feature tracking, and interferometry. A summary of the techniques, and what needs to be considered on a practical level, is provided in Table 1.

Manual survey

Manual surveys of glacier movement can be undertaken using a total station, theodolite or a dGPS to survey stakes inserted perpendicular into the glacier surface. The latter can achieve centimetre accuracy but access is required to the survey locations for all methods. The technique requires repeat measurements of stake positions so that the horizontal and vertical change between them can be calculated. Where debris is thick, a cross on a large boulder could be surveyed instead of stakes. Hubbard and Glasser (2005) provide a useful summary of surveying techniques and a method of transforming survey coordinates into velocities.

Manual survey methods require travel to the glacier itself, and then access to appropriate survey locations, which is time consuming and often hazardous on debris covered glaciers, and may not be possible on heavily crevassed clean ice glaciers. Therefore the spatial distribution of measurements is likely to be sparse, is dependent upon the preservation of the stakes between surveys, and is temporally limited to the duration and revisit period between field campaigns. It does however allow the simultaneous quantification of surface elevation change and glacier velocity (e.g. Pattyn *et al*., 2003; Zhang *et al.*, 2010; Zhang *et al.*, 2011). This is important on debris covered glaciers where the dominant response to climatic warming is often surface lowering, rather than terminus retreat (Benn *et al.*, 2012). Cavity uplift also produces vertical glacier movement, related to seasonally high subglacial water pressures and development of the glacier drainage system (e.g. Iken *et al.*, 1983; Hooke *et al.*, 1989; Mair *et al.*, 2002; Bingham *et al.*, 2006). Further information on the relationship between glacier strain and vertical velocity, and the calculation of cavity uplift velocities can be found in Iken *et al.* (1983) and Hooke *et al.* (1989). Assessments of vertical change are therefore essential and are otherwise limited by the high uncertainty often accompanying alternative remotely sensed geodetic DEM differencing methods (Racoviteanu *et al.*, 2008). Point-based measurements are also used to validate remote sensing derived velocity fields (e.g. Quincey *et al.*, 2009b; Herman *et al.*, 2011).

Uncertainty

Three types of error associated with total station/theodolite surveys are discussed by Copland *et al.* (2003). Briefly they are: positional error from determining the location of a stake; a displacement error between two stake surveys (e.g. the sum of positional errors); and, a velocity error, which is the displacement error adjusted for the time interval between surveys. A longer measurement interval reduces the overall velocity error; hence measurements may be subsampled over longer time periods. Mean velocity errors observed by Copland *et al.* (2003) were ± 1.1cm d^{-1} in the horizontal, and ± 0.6 cm d^{-1} in the vertical.

Uncertainty in dGPS surveys occurs from instrument error of the device and the field setup. For glacier movement applications (e.g. Quincey *et al.*, 2009a), the base station is mounted on stable ground off-glacier, and roving stations are either mounted permanently in the area of interest or used to survey locations intermittently (e.g. stakes or ground control points). The accuracy of a roving survey depends on the occupation time of the unit at each location, and satellite and atmospheric conditions, including the line of site to the base station (Hubbard and Glasser, 2005). Care is also required to maintain a stable antenna rod inclination during each occupation. Horizontal accuracy on the order of centimetres is achievable using a roving survey (e.g. Whitehead *et al.,* 2014). Achieving sub-centimetre accuracy comparable to that of a static survey requires long survey occupation times. However, such precision may not be practical or required.

Time-lapse camera survey

Using a time lapse camera array to observe glacier movement allows continuous data collection between field visits, in addition to ancillary information such as local weather conditions. The camera is used similarly to a theodolite, measuring the horizontal and

vertical trace lines from reference targets to the camera lens, whilst correcting for small camera movements using reference points on stable ground (Harrison *et al.,* 1992).

Implementation

3D point clouds can be automatically generated from photographs taken at different locations using Structure-from-Motion software (e.g. Westoby *et al.*, 2012), allowing both vertical and horizontal displacements to be quantified multi-temporally. This typically requires ca. >7 photographs of the subject taken from different locations (Micheletti *et al.,* 2014). For fewer cameras typical of a time-lapse array, surface movement in 3D space can be determined using traditional photogrammetry applied to cameras observing the glacier surface from an elevated position (e.g. Whitehead *et al.,* 2014). Whitehead *et al.* (2014) used 0.6 m diameter red circles on a white background as reference targets which were GPS surveyed to establish the coordinate system and reference frame. Daily X, Y, and Z position for targets can then be calculated using the multi-temporal imagery.

Uncertainty

Using a 39 Megapixel camera taking photos every ca. 10 minutes, Maas *et al.* (2008) achieved glacier displacement measurements accurate to several centimetres at distances of up to 5 km from the camera. Whitehead *et al.* (2014) achieved target positions of < 0.1 m at up to 800 m using two 10 Megapixel cameras. Glacier velocity was resolved up to 4 km from a 10.2 Megapixel camera set-up by Ahn and Box (2010). Here, for the Jakobshavn Isbræ averaging 37.6 m d^{-1} the displacement uncertainty was 2 %, whereas the slower moving Umiamako (5.9 m d^{-1}) averaged an uncertainty of 9 %. Uncertainty is related to glacier velocity, since positional uncertainty forms a lower proportion of an overall larger displacement.

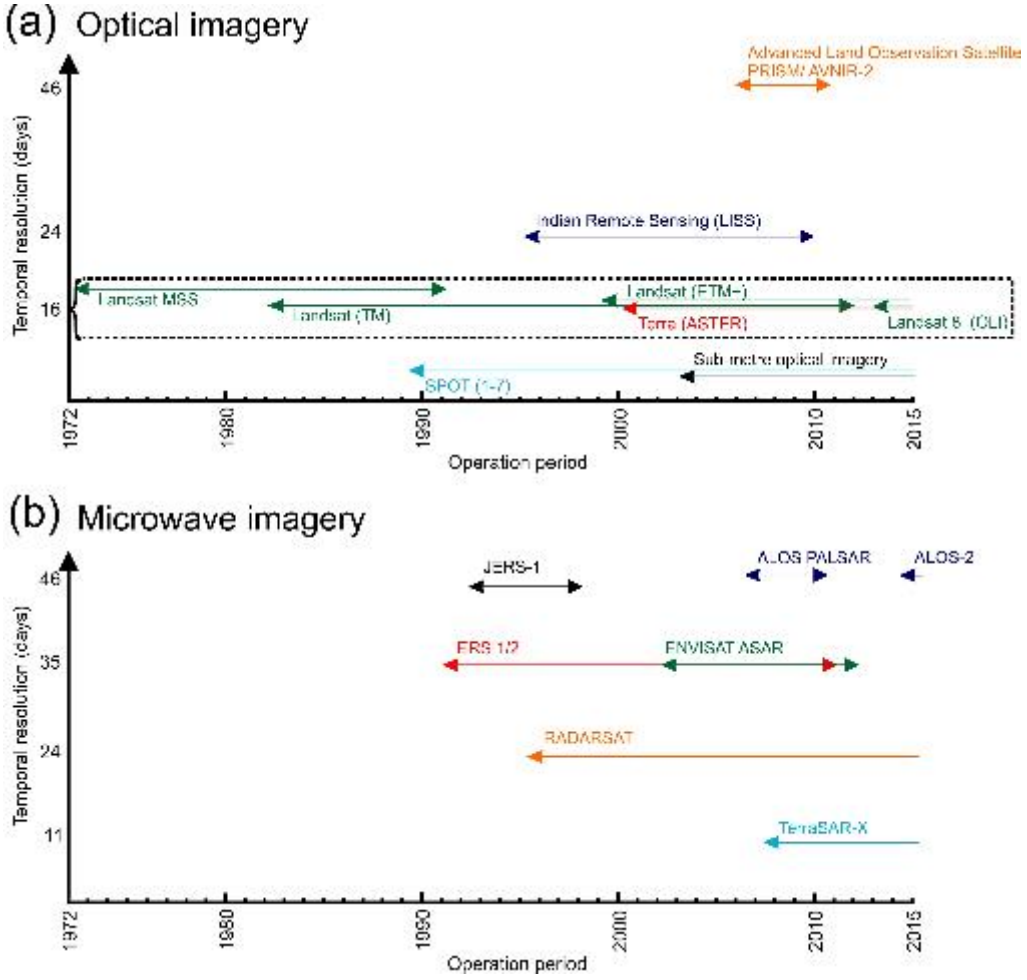

Figure 2. Typical optical and microwave imagery suitable for feature tracking applications. Actual archive coverage varies between regions. The Landsat and Terra (ASTER) archives have a 16 day repeat cycle (dashed box on (a)).

Feature tracking

Automated feature tracking using cross-correlation algorithms can generate spatially distributed velocity fields using multi-temporal optical or microwave remotely sensed imagery (Figure 2, Table 2). The software is used to extract features (e.g. boulders or debris patterns) from multiple images and the movement of the features is used to generate velocity fields. In addition to a greatly increased spatial density of measurements, feature tracking algorithms offer improved accuracy over manual feature tracking using remotely sensed imagery (e.g. Holt *et al.,* 2013), since the images can be co-registered to sub-pixel accuracy before analysis. Feature tracking relies on the preservation of features between scenes, such as boulders or debris patterns and crevasses (Strozzi *et al.,* 2002; Luckman *et al.,* 2003). Its suitability is therefore determined by the imagery resolution and revisit period, relative to glacier displacement between scenes. This can limit its application to fast moving (10s m d^{-1}) glaciers (Maas *et al.,* 2008), where sufficient temporal resolution imagery is not available or would be prohibitively expensive to obtain.

Implementation

Optimum optical input imagery should have the same sun angle and azimuth, and image viewpoint, such that surface features are similarly represented between scenes (Scambos *et al.,* 1992). For Landsat imagery this can be achieved using the same path and row locations for imagery collected at a similar time of year. Here, the finest resolution 15 m panchromatic band is likely to be used. However, where the panchromatic band is saturated, a combination of several bands may offer the best performance (e.g. Dehecq *et al.,* 2015). When using ASTER imagery, Redpath *et al.* (2013) observed the best performance with band 1 and the worst with band 3, attributed to enhanced band 1 contrast on the debris covered Tasman Glacier. The time interval between imagery should reflect the expected glacier velocity, such that surface features will have moved several pixels. A larger time interval therefore reduces uncertainty up to a threshold point, beyond which deformation in surface features between scenes will act to increase the uncertainty in establishing a match (Scambos *et al.,* 1992). Derived velocity fields require post-processing to remove spurious points and those that do not conform to the expected glacier flow direction or speed (Redpath *et al.,* 2013; Raup *et al.,* 2007) (Figure 3). Here thresholds for exclusion based on the correlation coefficient and signal to noise ratio can be set.

Optical vs. microwave imagery

Feature tracking techniques can also be implemented on SAR imagery (e.g. Strozzi *et al.*, 2002; Luckman *et al.*, 2007; Quincey *et al.*, 2009b) (Figure 2). SAR imagery does not require cloud free conditions to be suitable for feature tracking, nor is it affected by varying solar illumination, in contrast to optical imagery. Therefore SAR imagery can produce a more consistent dataset for monitoring glacier velocity (Luckman *et al.*, 2003, 2007), where surface features are distinctly visible over image speckle (noise). The procedure uses the same principle of cross-correlating features in image patches between scenes to determine glacier displacement as for optical imagery (Scambos *et al.,* 1992). In cases where coherence (phase of the received signal) is maintained between image pairs, the speckle can also be tracked on a finer scale to yield a displacement field.

Uncertainty

Errors in glacier displacement are associated with changes in the tracked surface features over the selected temporal resolution, geometric transformations of the data, and error in the location of stable reference points, which should be selected to exhibit zero displacement (e.g. bedrock outcrops) (Luckman *et al.*, 2007). Over shorter time periods (e.g. 1 day) the associated uncertainties are larger than compared with a longer (e.g. 35 day) period, where Luckman *et al.* (2003) estimated errors at ca. 1 m d^{-1} and ca. 0.03 m d^{-1} respectively using European Remote Sensing (ERS) satellite SAR imagery applied to several outlet glaciers in East Greenland. Error was reported to be sub-centimetre per day when applied to Himalayan glaciers by Luckman *et al.* (2007), and 1/20 of a pixel in the study of Strozzi *et al.* (2002).

Table 2. Examples of the software and techniques available for determining glacier velocity.

Method	Application	Glacial examples	Details
Feature tracking	CIAS software (2000) Optical imagery	Redpath *et al.* (2013)	Velocity fields were derived for the Tasman glacier 2009-2010, 2010-2011. Good agreement was observed between GPS measured and satellite derived velocities (R^2 = 0.97). ASTER band 1 was shown to offer the best performance for the debris covered glacier, and band 3N the worst (RMSE of 16.5 m a^{-1} and 60.1 m a^{-1} respectively)
		Kääb *et al.* (2005)	Landsat 7 ETM+ pan band and ASTER 3N band were used to derive velocity fields for the Kronebreen Glacier, Svalbard. Optical imagery feature tracking performed well over higher velocity areas. Interferometric synthetic aperture radar (InSAR) data were most suitable where optical contrast was low (e.g. over snow cover)
	COSI-Corr software (2007) Optical imagery	Herman *et al.* (2011)	ASTER band 3N imagery separated by 16 days was used to derive glacier velocities for an area of the Southern Alps, New Zealand. Velocities up to ca. 5 m d^{-1} were observed with uncertainties of ca 0.19 m d^{-1}. Comparison with ground dGPS measurements revealed large discrepancies where displacements were small (e.g. in accumulation areas)
		Scherler *et al.* (2008)	Glacier-surface velocities were derived from ASTER imagery for two Himalayan glaciers. A quality assessment methodology was demonstrated to improve measurement accuracy. Displacement error was on the order of 2–4 m per correlation
	ImGRAFT software (2014) Time-lapse imagery	Messerli and Grinsted (2015)	The image georectification and feature tracking toolbox (ImGRAFT) tailored for terrestrial oblique imagery was tested on time lapse imagery of the Engabreen Glacier icefall, Norway. A fine resolution DEM (e.g. laser scan) was required for georectification. The imagery revealed local flow characteristics, including extensional and compressional flow in the ice fall
	Satellite radar feature tracking (SRFT). Radar imagery	Luckman *et al.* (2007)	Repeat pass satellite radar imagery allowed glacier surface patterns to be tracked between scenes. Scene separations of 245 – 1890 days. Suggested error of < 0.5 cm d^{-1} over the study period. The technique was most suitable on slow moving, debris-covered glacier areas
	Manual feature tracking. Optical imagery	Immerzee *et al.* (2014)	Manual feature tracking was used to create a velocity field for the Lirung Glacier, Nepal using a ca. 5 cm resolution DEM derived from Unmanned Aerial Vehicle (UAV) surveys in May and October 2013. Distinguishable features (e.g. boulders) (n = 145) were identified on multi-temporal ortho-mosaics and used to calculate horizontal displacement
SAR interferometry	GAMMA SAR software	Quincey *et al.* (2007)	SAR interferometry was applied to five Himalayan debris-covered glaciers and provided a spatial resolution (< 20 m^2) and errors of less than 0.01 m d^{-1} for a pair of ERS-1/2 images from 29–30 March 1996. Supraglacial lake development was associated with areas of low glacier displacement
		Schneevoigt *et al.* (2012)	Glacier displacement was derived for Comfortlessbreen, Svalbard, using SAR interferometry applied to ERS-1/-2 scenes from April and May 1996. This provided a pre-surge velocity baseline
dGPS	Stake survey	Herman *et al.* (2011)	Crevassing restricted longitudinal stake coverage during the manual survey. A maximum horizontal error of 0.2 m was suggested between stake surveys (2002-2006). dGPS measurements also revealed vertical glacier surface changes
	Stake survey	Kirkbride and Deline (2013)	Ablation stakes were surveyed annually (2005 – 2008) on the Glacier d'Estelette, Itlay, to characterise surface debris transport. Surveying was conducted using a dGPS in real-time stop-and-go mode, which lead to mean positional errors of 0.031 m in the horizontal and 0.026 m in the vertical
Theodolite / total station	Stake survey	Copland *et al.* (2003)	34 stakes were surveyed in the lower 3 km of the John Evans Glacier in 1998. Reflecting prisms were mounted on the 3 m stakes which were drilled into the glacier surface. Each stake was surveyed daily from two independent locations using a total station theodolite
	Stake survey	Mair *et al.* (2008)	13 stakes placed on the Haut Glacier d'Arolla, Switzerland, were surveyed over 10 days using a total station situated on a moraine to determine diurnal velocity variation. Two-hourly surveys were also conducted for a three-day period during daylight hours. Stakes were located to within ±3-5 mm which translated into velocity errors of < ±0.04 m d^{-1} when averaged over two hour intervals. Diurnal variability was observed during the two-hourly surveys, although this was on the order of measurement uncertainty

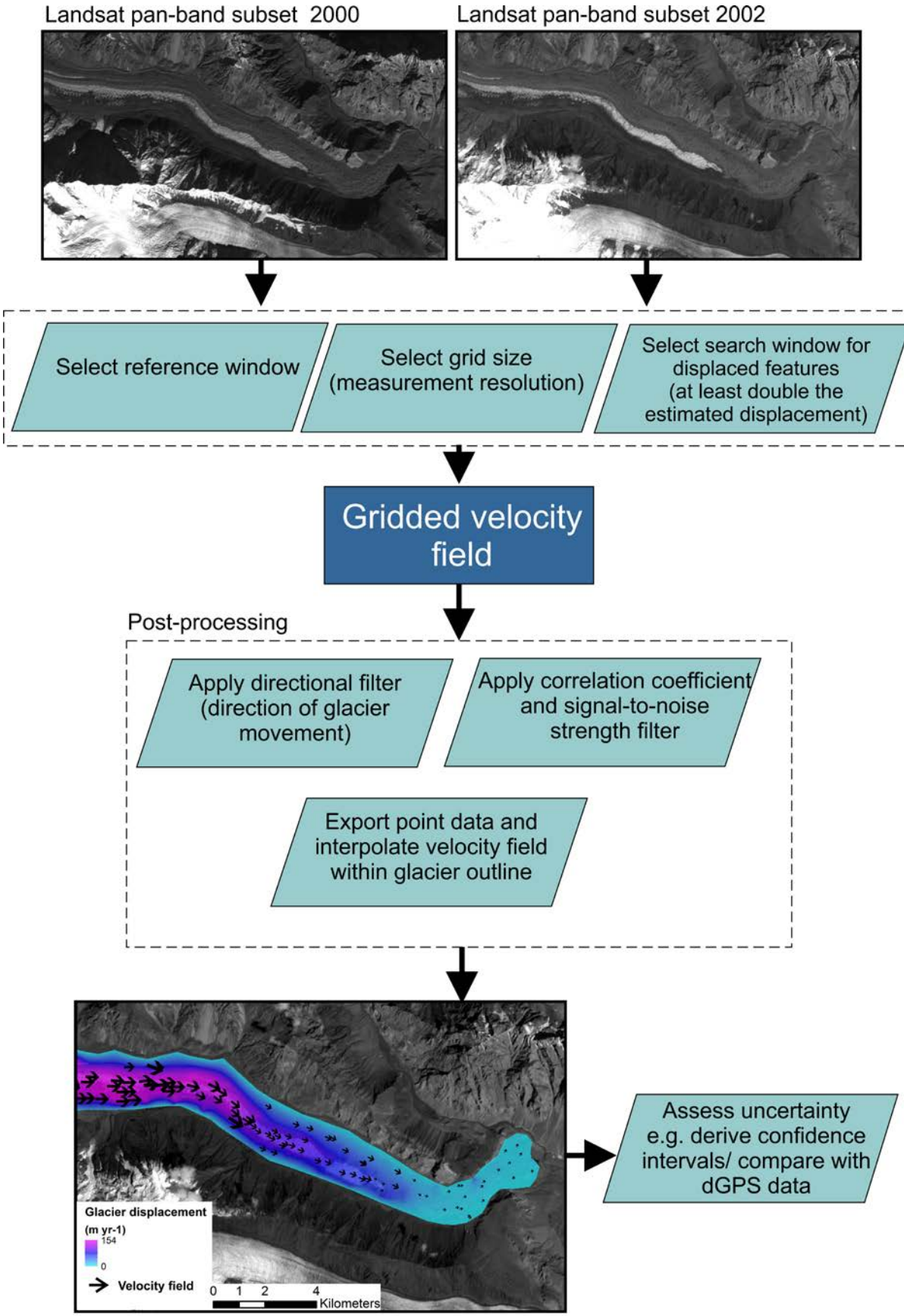

Figure 3. A typical feature tracking workflow for deriving glacier velocity. This example used Landsat 7 ETM+ *panchromatic scenes of the Batura Glacier and CIAS software, both available from: http://www.mn.uio.no/geo/english/research/projects/icemass/cias*

SAR interferometry

SAR interferometry reveals glacier displacement represented through fringe patterns, which correspond to surface displacement (e.g. Figure 4). The process requires coherence to be maintained between images (Massonnet and Feigl, 1998). Coherence can be lost because of:

1. too much displacement between acquisitions due to rapid ice flow or a long satellite revisit period.
2. a change in surface appearance due to surface melt or fresh snow cover.

The requirement of preserved coherence usually limits InSAR measurements to diurnal velocities, which can be beneficial for seasonal or short-term patterns, but becomes unrepresentative if scaled up to annual or longer-term periods. In this case, feature tracking techniques can be beneficial (Strozzi *et al.*, 2002). However, where both short–term and annually averaged velocities are required, both SAR interferometry and feature tracking can be used as complementary methods (e.g. Quincey *et al.*, 2009b).

Implementation

The workflow for deriving glacier displacement using interferometry is outlined in Figure 5 and is extensively reviewed by Massonnet and Feigl (1998), summarised here. In brief, SAR interferometry requires the images to be finely co-registered so that an interferogram can be produced. This represents, on a pixel by pixel basis, the phase difference between the received signals from each image. This phase difference is dependent on surface topography, the positions of the sensors at the time of image acquisition, a signal relating to the curvature of the Earth, and any surface displacement that has occurred on the ground. The signals relating to the first three of these factors can be simulated (or measured) and then removed from the overall phase to leave only that relating to surface displacement. The remaining glacier displacement signal is then unwrapped from a known stationary point to create a velocity

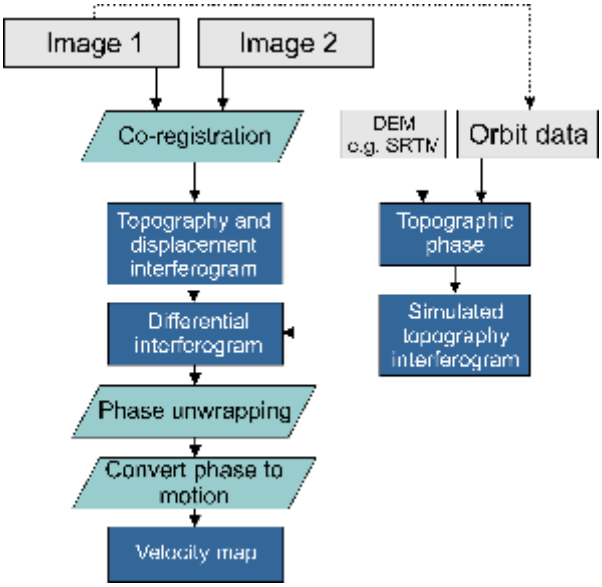

Figure 5. SAR interferometry processing workflow to calculate glacier velocity. Adapted from Rao (2014).

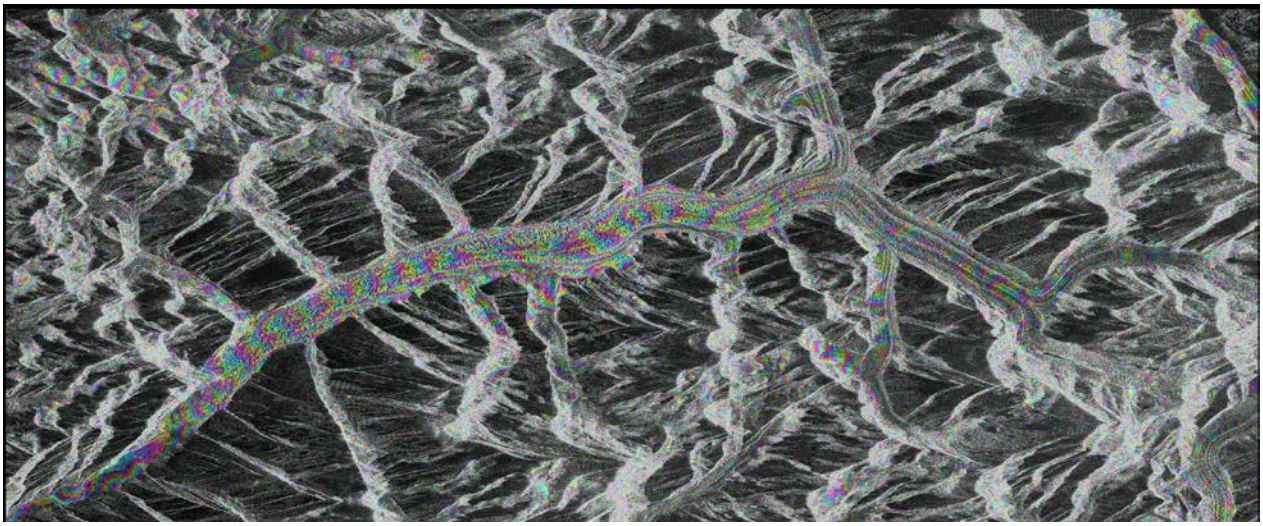

Figure 4. An example interferogram of the Baltoro Glacier. Coloured fringes represent glacier movement.

map, although it should be noted that any vertical surface change (e.g. subsidence, surface melt) will also be incorporated in the final velocity data. Displacements that can be measured are normally of the order of the wavelength of the imagery (i.e. cm's).

Conclusion

dGPS surveying techniques can afford greater precision compared to feature tracking methods but measurements are restricted both spatially and temporally, dictated by site accessibility and field costs. However, dGPS measurements also quantify vertical displacement, important on downwasting debris-covered glaciers, or when assessing cavity uplift. The increasing use of time-lapse imagery can be exploited with semi-automated techniques to derive glacier velocity and reveal local displacement characteristics, whilst also resolving displacements at centimetre resolution at hundreds of metres from the camera positions.

Recent computational developments have allowed spatially distributed velocity fields to be calculated for multiple glaciers with relative ease and with high accuracy, using a wide range of optical and SAR remotely sensed imagery. Feature tracking and SAR interferometry can be used to obtain annually averaged and short-term velocity fields respectively, such that the techniques can be complementary. The greater availability of datasets and broader applicability to both debris-covered and clean-ice glaciers tends towards greater application of feature tracking methods, although interferometry has the clear advantage of being able to yield velocity data over largely featureless surfaces. In either case, use of remotely-sensed imagery allows glacier velocity to be derived for crevassed and other inaccessible areas of the glacier, which cannot be otherwise obtained using manual surveying techniques.

As remote sensing imagery archives continue to expand, observations of glacier velocity will increasingly complement assessments of mass balance. This allows a more integrated assessment of glacier dynamics to assess the response to climate change and other internal feedback mechanisms. This is especially pertinent at lacustrine- and marine-terminating glaciers where interplay between glacier mass export and calving exists, and also on debris-covered glaciers where surface morphology and glacial lake development are closely linked to glacier stagnation.

Acknowledgements

We thank two reviewers and the editor, Lucy Clarke, whose comments helped improve this article.

References

Ahn Y and Box JE. 2010. Glacier velocities from time-lapse photos: technique development and first results from the Extreme Ice Survey (EIS) in Greenland. *Journal of Glaciology.* **56**: 723-734.

Benn DI, Bolch T, Hands K, Gulley J, Luckman A, Nicholson LI, Quincey D, Thompson S, Toumi R and Wiseman S. 2012. Response of debris-covered glaciers in the Mount Everest region to recent warming, and implications for outburst flood hazards. *Earth-Science Reviews.* **114**: 156-174.

Benn DI and Evans DJA. 2010. *Glaciers and glaciation.* London: Hodder Education.

Benn DI and Owen LA. 2002. Himalayan glacial sedimentary environments: a framework for reconstructing and dating the former extent of glaciers in high mountains. *Quaternary International.* **97-8**: 3-25.

Bingham RG, King EC, Smith AM and Pritchard HD. 2010. Glacial geomorphology: Towards a convergence of glaciology and geomorphology. *Progress in Physical Geography.* **34**: 327-355.

Bingham RG, Nienow PW, Sharp MJ and Copland L. 2006. Hydrology and dynamics of a polythermal (mostly cold) High Arctic glacier. *Earth Surface Processes and Landforms.* **31**: 1463-1479.

Bolch T, Kulkarni A, Kääb A, Huggel C, Paul F, Cogley JG, Frey H, Kargel JS, Fujita K, Scheel M, Bajracharya S and Stoffel M. 2012. The State and Fate of Himalayan Glaciers. *Science.* **336**: 310-314.

Clarke GKC, Collins SG and Thompson DE. 1984. Flow, thermal structure, and subglacial conditions of a surge-type glacier. *Canadian Journal of Earth Sciences.* **21**: 232-240.

Copland L, Sharp MJ and Nienow PW. 2003. Links between short-term velocity variations and the subglacial hydrology of a predominantly cold polythermal glacier. *Journal of Glaciology.* **49**: 337-348.

Dehecq A, Gourmelen N and Trouve E. 2015. Deriving large-scale glacier velocities from a complete satellite archive: Application to the Pamir–Karakoram–Himalaya. *Remote Sensing of Environment.* **162**: 55-66.

Evans DJA, Clark CD and Mitchell WA. 2005. The last British Ice Sheet: A review of the evidence utilised in the compilation of the Glacial Map of Britain. *Earth-Science Reviews.* **70**: 253-312.

Evans DJA and Rea BR. 1999. Geomorphology and sedimentology of surging glaciers: a land-systems approach. *Annals of Glaciology.* **28**: 75-82.

Gardelle J, Berthier E, Arnaud Y and Kaab A. 2013. Region-wide glacier mass balances over the Pamir-Karakoram-Himalaya during 1999-2011. *Cryosphere.* **7**: 1263-1286.

Hambrey MJ, Quincey DJ, Glasser NF, Reynolds JM, Richardson SJ and Clemmens S. 2008. Sedimentological, geomorphological and dynamic context of debris-mantled glaciers, Mount Everest (Sagarmatha) region, Nepal. *Quaternary Science Reviews.* **27**: 2361-2389.

Harrison WD, Echelmeyer KA, Cosgrove DM and Raymond CF. 1992. The determination of glacier speed by time-lapse photography under unfavorable conditions. *Journal of Glaciology.* **38**: 257-265.

Herman F, Anderson B and Leprince S. 2011. Mountain glacier velocity variation during a retreat/advance cycle quantified using sub-pixel analysis of ASTER images. *Journal of Glaciology.* **57**: 197-207.

Holt TO, Glasser NF, Quincey DJ and Siegfried MR. 2013. Speedup and fracturing of George VI Ice Shelf, Antarctic Peninsula. *The Cryosphere.* **7**: 797-816.

Hooke RL, Calla P, Holmlund P, Nilsson M and Stroeven A. 1989. A three year record of seasonal variations in surface velocity, Storglaciären, Sweden. *Journal of Glaciology.* **35**: 235-247.

Hubbard B. 2002. Direct measurement of basal motion at a hard-bedded, temperate glacier: Glacier de Tsanfleuron, Switzerland. *Journal of Glaciology.* **48**: 1-8.

Hubbard B and Glasser NF. 2005. *Field techniques in glaciology and glacial geomorphology.* Chichester: John Wiley.

Iken A, Rothlisberger H, Flotron A and Haeberli W. 1983. The uplift of Unteraargletscher at the beginning of the melt season – a consequence of water storage at the bed. *Journal of Glaciology.* **29**: 28-47.

Immerzeel WW, Kraaijenbrink PDA, Shea JM, Shrestha AB, Pellicciotti F, Bierkens MFP and de Jong SM. 2014. High-resolution monitoring of Himalayan glacier dynamics using unmanned aerial vehicles. *Remote Sensing of Environment.* **150**: 93-103.

Kääb A, Lefauconnier B and Melvold K. 2005. Flow field of Kronebreen, Svalbard, using repeated Landsat 7 and ASTER data. In: Dowdeswell, J. and Willis, I.C. eds. *Annals of Glaciology, Vol 42, 2005.* pp.7-13.

Kamb B, Raymond CF, Harrison WD, Engelhardt H, Echelmeyer KA, Humphrey N, Brugman MM and Pfeffer T. 1985. Glacier Surge Mechanism: 1982-1983 Surge of Variegated Glacier, Alaska. *Science.* **227**: 469-479.

Kavanaugh JL and Clarke GKC. 2006. Discrimination of the flow law for subglacial sediment using in situ measurements and an interpretation model. *Journal of Geophysical Research-Earth Surface.* **111**.

Kirkbride MP and Deline P. 2013. The formation of supraglacial debris covers by primary dispersal from transverse englacial debris bands. *Earth Surface Processes and Landforms.* **38**: 1779-1792.

Kodama H and Mae S. 1976. The Flow of Glaciers in the Khumbu Region. Glaciological Expedition to Nepal, Contribution No. 10. *Journal of the Japanese Society of Snow and Ice.* **38**: 31-36.

Luckman A, Murray T, Jiskoot H, Pritchard H and Strozzi T. 2003. ERS SAR feature-tracking measurement of outlet glacier velocities on a regional scale in East Greenland. *Annals of Glaciology.* **36**: 129-134.

Luckman A, Quincey D and Bevan S. 2007. The potential of satellite radar interferometry and feature tracking for monitoring flow rates

of Himalayan glaciers. *Remote Sensing of Environment.* **111**: 172-181.

Maas H-G, Schwalbe E, Dietrich R, Bässler M and Ewert H. 2008. Determination of spatio-temporal velocity fields on glaciers in West-Greenland by terrestrial image sequence analysis. *International Archives of Photogrammetry, Remote Sensing and Spatial Information Science.* **37**: 1419-1424.

Mair D, Hubbard B, Nienow P, Willis I and Fischer UH. 2008. Diurnal fluctuations in glacier ice deformation: Haut Glacier d'Arolla, Switzerland. *Earth Surface Processes and Landforms.* **33**: 1272-1284.

Mair DWF, Sharp MJ and Willis IC. 2002. Evidence for basal cavity opening from analysis of surface uplift during a high-velocity event: Haut Glacier d'Arolla, Switzerland. *Journal of Glaciology.* **48**: 208-216.

Mair D, Nienow P, Willis I and Sharp M. 2001. Spatial patterns of glacier motion during a high-velocity event: Haut Glacier d'Arolla, Switzerland. *Journal of Glaciology.* **47**: 9-20.

Massonnet D and Feigl KL. 1998. Radar interferometry and its application to changes in the earth's surface. *Reviews of Geophysics.* **36**: 441-500.

Meier MF and Post A. 1969. What are glacier surges? *Canadian Journal of Earth Sciences.* **6**: 807-817.

Messerli A and Grinsted A. 2015. Image georectification and feature tracking toolbox: ImGRAFT. *Geosci. Instrum. Method. Data Syst.* **4**: 23-34.

Micheletti N, Chandler JH and Lane SN. 2014. Investigating the geomorphological potential of freely available and accessible structure-from-motion photogrammetry using a smartphone. *Earth Surface Processes and Landforms.* n/a-n/a.

Nesje A. 2009. Latest Pleistocene and Holocene alpine glacier fluctuations in Scandinavia. *Quaternary Science Reviews.* **28**: 2119-2136.

Quincey DJ, Braun M, Glasser NF, Bishop MP, Hewitt K and Luckman A. 2011. Karakoram glacier surge dynamics. *Geophysical Research Letters.* **38**: L18504.

Quincey DJ, Copland L, Mayer C, Bishop M, Luckman A and Belò M. 2009a. Ice velocity and climate variations for Baltoro Glacier, Pakistan. *Journal of Glaciology.* **55**: 1061-1071.

Quincey DJ, Luckman A and Benn D. 2009b. Quantification of Everest region glacier velocities between 1992 and 2002, using satellite radar interferometry and feature tracking. *Journal of Glaciology.* **55**: 596-606.

Quincey DJ, Richardson SD, Luckman A, Lucas RM, Reynolds JM, Hambrey MJ and Glasser NF. 2007. Early recognition of glacial lake hazards in the Himalaya using remote sensing datasets. *Global and Planetary Change*. **56**: 137-152.

Quincey DJ, Lucas RM, Richardson SD, Glasser NF, Hambrey MJ and Reynolds JM. 2005. Optical remote sensing techniques in high-mountain environments: application to glacial hazards. *Progress in Physical Geography.* **29**: 475-505.

Racoviteanu AE, Williams MW and Barry RG. 2008. Optical remote sensing of glacier characteristics: A review with focus on the Himalaya. *Sensors.* **8**: 3355-3383.

Rao YS. 2014. Synthetic Aperture Radar (SAR) Interferometry for Glacier Movement Studies. In: Singh, V.Singh, P. and Haritashya, U. eds. *Encyclopedia of Snow, Ice and Glaciers.* Springer Netherlands, pp.1133-1142.

Raup B, Kaab A, Kargel JS, Bishop MP, Hamilton G, Lee E, Paul F, Rau F, Soltesz D, Khalsa SJS, Beedle M and Helm C. 2007. Remote sensing and GIS technology in the global land ice measurements from space (GLIMS) project. *Computers & Geosciences.* **33**: 104-125.

Redpath TAN, Sirguey P, Fitzsimons SJ and Kääb A. 2013. Accuracy assessment for mapping glacier flow velocity and detecting flow dynamics from ASTER satellite imagery: Tasman Glacier, New Zealand. *Remote Sensing of Environment.* **133**: 90-101.

Reid TD and Brock BW. 2014. Assessing ice-cliff backwasting and its contribution to total ablation of debris-covered Miage glacier, Mont Blanc massif, Italy. *Journal of Glaciology.* **60**: 3-13.

Sakai A, Nakawo M and Fujita K. 2002. Distribution characteristics and energy balance of ice cliffs on debris-covered glaciers, Nepal Himalaya. *Arctic Antarctic and Alpine Research.* **34**: 12-19.

Scambos TA, Dutkiewicz MJ, Wilson JC and Bindschadler RA. 1992. Application of image cross-correlation to the measurement of glacier velocity using satellite image data. *Remote Sensing of Environment.* **42**: 177-186.

Schneevoigt NJ, Sund M, Bogren W, Kaab A and Weydahl DJ. 2012. Glacier displacement on Comfortlessbreen, Svalbard, using 2-pass differential SAR interferometry (DInSAR) with a digital elevation model. *Polar Record.* **48**: 17-25.

Strozzi T, Luckman A, Murray T, Wegmuller U and Werner CL. 2002. Glacier motion estimation using SAR offset-tracking procedures. *Geoscience and Remote Sensing, IEEE Transactions on.* **40**: 2384-2391.

Westoby MJ, Glasser NF, Brasington J, Hambrey MJ, Quincey DJ and Reynolds JM. 2014. Modelling outburst floods from moraine-dammed glacial lakes. *Earth-Science Reviews.* **134**: 137-159.

Westoby MJ, Brasington J, Glasser NF, Hambrey MJ and Reynolds JM. 2012. 'Structure-from-Motion' photogrammetry: A low-cost, effective tool for geoscience applications. *Geomorphology.* **179**: 300-314.

Whitehead K, Moorman B and Wainstein P. 2014. Measuring daily surface elevation and velocity variations across a polythermal arctic glacier using ground-based photogrammetry. *Journal of Glaciology.* **60**: 1208-1220.

Zwally HJ, Abdalati W, Herring T, Larson K, Saba J and Steffen K. 2002. Surface Melt-Induced Acceleration of Greenland Ice-Sheet Flow. *Science.* **297**: 218-222.